Holography in commercially available photoetchable glasses

Michael Kösters, Hung-Te Hsieh, Demetri Psaltis, and Karsten Buse

Volume holographic gratings are recorded and retrieved in two commercially available glasses: Schott Foturan and Hoya PEG3. These materials are photoetchable, which describes their major application, but they also allow storage of volume holograms without any chemical etching. The samples are illuminated with ultraviolet light at a wavelength of 325 nm and thermally processed to achieve a maximum diffraction efficiency of ≈9% for a 1-mm-thick sample. The two glasses show similar behavior; the diffraction efficiencies in Foturan tend to be slightly larger, whereas PEG3 tends to have weaker light scattering.

OCIS codes: 090.7330, 090.2900.

1. Introduction

Volume holograms are useful for applications such as wavelength filters in optical telecommunication networks and holographic data storage.[1,2] Robust recording materials with excellent long-term stability of the written holograms are a requirement for such applications. Here we present a study of the holographic properties of two commercially available photoetchable glasses, Foturan from Schott and PEG3 from Hoya. These glasses also allow for the storage of volume holograms by illumination with UV light and a subsequent annealing procedure, but without any chemical etching. Thus it is expected that these glasses are useful as holographic recording media.

The photoetchable glasses examined in this paper are cerium–silver-doped lithium–aluminum–silicate glasses. Changes of the refractive index and of the absorption are obtained as described by the following relations[3]:

$$\text{Irradiation}: \ \mathrm{Ce}^{3+} \xrightarrow{\lambda=325\ \mathrm{nm}} \mathrm{Ce}^{4+} + e^{-}, \tag{1}$$

$$1.\ \text{Annealing}: \ n\mathrm{Ag}^{+} + ne^{-} \rightarrow (\mathrm{Ag})_n, \tag{2}$$

$$2.\ \text{Annealing}: \ (\mathrm{Ag})_n \ \text{as seed crystals} \ \rightarrow \ \text{lithium metasilicate, causes refractive-index and absorption changes.} \tag{3}$$

By illumination with UV light (in our case with light at a wavelength $\lambda = 325$ nm), the cerium is oxidized from the 3+ state to the 4+ state releasing one electron. In a first annealing step the released electrons reduce the positively charged silver ions. The neutral silver atoms have a high mobility; they move and form silver clusters within the glass. In a second annealing step at a higher temperature, these silver clusters act as seed crystals for the crystallization of the glass around them. It is this crystallization that produces the main refractive-index and absorption changes. For suitable annealing temperatures and times, the crystals do not approach or exceed the dimension of the light wavelength, and hence light scattering is weak. Such glasses have been tailored and tested for holographic and other optical applications,[4,5] but here our aim is to evaluate commercially available photoetchable glasses with regard to their holographic properties and to maximize the diffraction efficiencies while keeping scattering around the readout wavelength as low as possible.

The photoetchable glasses Foturan and PEG3 have the compositions shown in Table 1.[6,7] Since they possess similar physical, chemical, and electrical properties, we expect them to show similar behavior.

M. Kösters (koesters@physik.uni-bonn.de), H.-T. Hsieh, and D. Psaltis are with the Department of Electrical Engineering, California Institute of Technology, Mail Stop 136-93, Pasadena, California 91125. K. Buse is with the Institute of Physics, University of Bonn, Wegelerstrasse 8, Bonn D-53115, Germany.

Received 25 October 2004; revised manuscript received 10 February 2005; accepted 11 February 2005.

0003-6935/05/173399-04$15.00/0

Table 1. Compositions of Foturan[a] and PEG3[b]

Compound	Symbol	Foturan (%)	PEG3 (%)
Silica	SiO_2	75–85	78
Lithium oxide	Li_2O	7–11	10
Aluminum oxide	Al_2O_3	3–6	6
Potassium oxide	K_2O	3–6	4
Sodium oxide	Na_2O	1–2	1
Zinc oxide	ZnO	0–2	1
Antimony oxide	Sb_2O_3	0.2–0.4	—
Silver oxide	Ag_2O	0.05–0.15	0.08
Cerium oxide	CeO_2	0.01–0.04	0.08
Gold oxide	AuO	—	0.003

[a]Ref. 6.
[b]Ref. 7.

2. Experimental Methods

The Foturan samples came in 1-mm-thick slices of 4.5 cm × 4.5 cm whereas the Hoya slices of PEG3 were 3 mm thick and 10 cm × 10 cm wide. After cutting, the samples used in the experiments had an area of ≈1 cm × 1 cm. The sample processing was done in two steps: an irradiation step to generate volume holograms and an annealing step to thermally develop and fix the holograms in the glass.

The setup for the holographic recording is shown in Fig. 1. A randomly polarized HeCd laser operating at the wavelength $\lambda = 325$ nm was used as the light source. The beam was expanded to ensure a more homogeneous illumination of the samples. The full width at half-maximum diameter of the recording beams was ≈8 mm. With the angle between the surface normal and the recording beams set to 15° (in the air), the resulting grating period length became $\Lambda = 0.6$ μm. As an alternative, in some experiments we projected a mask onto the samples instead of using the interference pattern. An intensity of 1.3 mW/cm^2 was used to generate exposures ranging from 2.5 to 15 J/cm^2.

The second processing step was thermal annealing. After a series of trials, we modified the annealing schedules suggested by the manufacturers to achieve optimum performance for the holographic application. We placed the samples in the oven and raised the temperature at a rate of ≈3–4 °C/min up to 500 °C (for Foturan) and 490 °C (for PEG3). This temperature was kept stable for periods of up to 2 h before the temperature was raised to 580–590 °C at a rate of ≈1–2 °C/min. Then the samples were either left there for up to 15 min or directly cooled down at a rate of ≈4 °C/min. The samples stood upright in the oven in the same orientation as in the illumination setup.

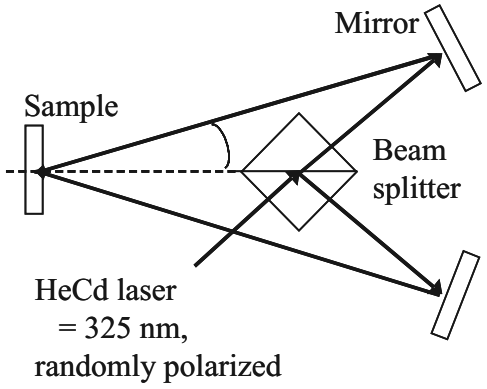

Fig. 1. Setup used for holographic recording.

To characterize the samples, laser light at several wavelengths ($\lambda = 633, 785, 840$ nm) was used to measure the diffraction. The measurements were taken by setting the samples onto a rotation stage. We recorded the diffracted light intensity I_{diff} versus the angle of incidence θ and measured the transmitted intensity I_{trans} at the Bragg angle; thereby we can calculate the diffraction efficiency using

$$\eta = \frac{I_{diff}}{I_{diff} + I_{trans}}. \quad (4)$$

The coupled-wave theory allows us to determine from $\eta(\theta)$ the effective thickness d of the volume holograms.[8] This d can be smaller than the actual thickness of the sample because of absorption. The holographic sample characterization was done after each processing step, meaning after the illumination and after the annealing.

3. Experimental Results

In general, the Foturan samples showed a mostly clear yellow-brownish color after the first annealing step. After the second step, the glass developed milky effects due to the crystallization and became more scattering.

The PEG3 samples showed colors varying from pink to brown and then yellow, depending on the exposure. The best holographic results were obtained with samples having a brown color at the center (and pink outer parts due to the Gaussian beam illumination), as is suggested in the Hoya product information for photoetchable applications. For those samples, milky effects appeared after the second annealing, but did not cause excessive scattering. Typical numbers for light scattering covered a very wide range from ≈1% of the incident intensity for the best samples to more than 90% for the worst samples.

Table 2 gives a short overview of some of the experimental results that are gained from Foturan as well as PEG3 samples. For each sample, the processing is given in terms of the exposure and the annealing conditions. The latter are divided into five parts: (a) the averaged heating rate for the first annealing step, (b) the time that the sample was kept at a stable temperature, (c) the rate to the final temperature of the second annealing step, (d) the waiting time at this final temperature, and (e) the cooling rate down to room temperature. The experimental results for the extinction α (including absorption and scattering), for η, and for the effective hologram thickness d are shown.

A typical fully processed Foturan sample has a

Table 2. Typical Sample Processing and Experimental Results for Foturan and PEG3[a]

Glass Type	Exposure	Annealing Conditions	Results: 633 nm	Results: 785 nm	Results: 840 nm
			α η d	α η d	α η d
Foturan	10 J/cm^2	(a) 3.2 °C/min to 500 °C (b) 120 min at 500 °C (c) 1.3 °C/min to 590 °C (d) — (e) ≈ 4 °C/min	0.73 mm^{-1} 0.6% 0.63 mm	0.27 mm^{-1} 0.25% 0.61 mm	0.27 mm^{-1} 0.21% 0.44 mm
	15 J/cm^2	(a) 3.5 °C/min (b) 120 min (c) 1.3 °C/min (d) — (e) ≈ 4 °C/min	4.31 mm^{-1} 9.4% 0.61 mm	2.24 mm^{-1} 3.9% 0.59 mm	1.87 mm^{-1} 6.3% 0.68 mm
PEG3	10 J/cm^2	(a) 3.5 °C/min to 490 °C (b) 90 min at 490 °C (c) 2.0 °C/min to 580 °C (d) — (e) ≈ 4 °C/min	0.24 mm^{-1} 0.55% 1.32 mm	0.11 mm^{-1} 0.36% 1.69 mm	0.07 mm^{-1} 0.13% 0.55 mm

[a]α, light extinction coefficient; η, diffraction efficiency; d, effective sample thickness.

diffraction efficiency of 0.2% (values given for a readout wavelength λ = 840 nm) accompanied by 0.27-mm^{-1} extinction and an effective grating thickness of ≈0.44 mm (example fit for λ = 633 nm; see Fig. 2).

Focusing more on the diffraction efficiency, the highest η measured for Foturan is ≈9.4%, but with an extinction coefficient α of 4.3 mm^{-1}. The Hoya glass PEG3 behaves similar to the Foturan from Schott. The optimized diffraction efficiencies are slightly lower for PEG3, but the extinction is also less. In PEG3, the effective grating thickness is larger than that in Foturan (see Table 2). These differences are relatively small and may be within the variability of our experiments.

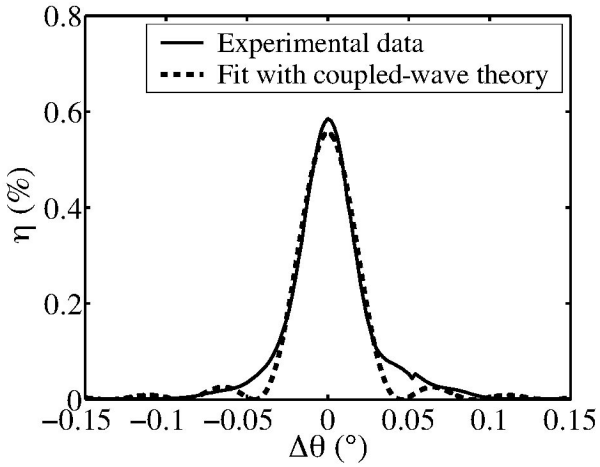

Fig. 2. Diffraction efficiency η versus readout angle Δθ = (θ − θ_B) for a Foturan sample at the readout wavelength λ = 633 nm. The dashed curve is a fit of the coupled-wave theory[8] to the experimental data (fit parameters d = 0.63 mm and the grating amplitude).

In some cases we also separated the two annealing steps and cooled the samples down to room temperature before heating them up to 580 °C. This separation does not lead to any considerable change of the final values for either the diffraction efficiency and extinction or the fit parameter d.

Experiments with 2-, 10-, and 50-μm masks lead to very strong gratings for the 10- and 50-μm masks with the first diffraction order as strong as the undiffracted beam. This gives a diffraction efficiency η ≈ 50%. The exposure was between 1–5 J/cm^2 and hence lower than the one in the holographic experiments.

In both cases—for the holographically recorded gratings as well as for those recorded with the masks—after thermal processing no degradation or fading of the holograms could be observed over several months of experiments.

4. Discussion

We were able to store volume holographic gratings in two commercially available photoetchable glasses: Foturan from Schott and Hoya PEG3.

The angular selectivity curve does not show a perfect sinc function as is expected from the coupled-wave theory.[8] This is probably caused by the effect that the glass absorbs the recording light, and hence the gratings are not homogeneous over the depth.

We do not have direct measurements that show whether phase or absorption gratings dominate. However, especially the experiments with the 50-μm mask and the resulting very high diffraction efficiencies make it most likely that the phase gratings also

dominate in the holographic experiments. From the coupled-wave theory[8] we then conclude that refractive-index changes of up to 2.5×10^{-5} are obtained. A beam-coupling experiment of a moving grating[9,10] could give information on which contribution to the diffraction efficiency is caused by amplitude and which is caused by phase gratings.

A further aspect that also deserves attention is the possibility of an effective shrinkage of the holograms upon thermal development: Physical contraction as well as homogeneous refractive-index changes may alter the Bragg condition. Nevertheless, it is evident that in inorganic glasses such effects will be much smaller than in photopolymers.

The experiments with the 2-, 10-, and 50-μm masks clearly show a trade-off between resolution and diffraction efficiency: As the holographic experiments prove, recording in the micrometer range is possible, but much stronger holograms are obtained with the 50-μm mask. Maybe this can be attributed to a long diffusion length in the recording or annealing process. This explanation is consistent with the observation that the 2-μm mask showed approximately the same results as the volume holography. Further experiments are needed to confirm this since the stability of the recording setup with the mask is better. Moreover, we find that with the mask the optimum exposure energies are lower.

In conclusion, our investigation shows that commercially available photoetchable glasses are an interesting holographic recording medium and that this material deserves further attention.

The authors thank M. Wengler for giving vital information on the experiments and the analysis. The research at Caltech was financially supported by the National Science Foundation Engineering Research Center and a German Academic Exchange Service scholarship.

References

1. P. Boffi, D. Piccinin, and M. C. Ubaldi, *Infrared Holography for Optical Communications* (Springer, Berlin, 2003).
2. H. J. Coufal, D. Psaltis, and G. T. Sincerbox, *Holographic Data Storage* (Springer, Berlin, 2000).
3. S. D. Stookey, "A new photographic medium," Ind. Eng. Chem. **41,** 856–861 (1949).
4. O. M. Efimov, L. B. Glebov, L. N. Glebova, K. C. Richardson, and V. I. Smirnov, "High-efficiency Bragg gratings in photothermorefractive glass," Appl. Opt. **34,** 619–627 (1999).
5. N. F. Borrelli, D. L. Morse, and P. A. Sachenik, "Integral photosensitive optical device and method," U.S. patent 4,514,053 (30 April 1985).
6. T. R. Dietrich, W. Ehrfeld, M. Lacher, M. Kraemer, and B. Speit, "Fabrication technologies for microsystems utilizing photoetchable glass," Microelectron. Eng. **30,** 497–504 (1996).
7. T. Fushie, T. Kagatsume, and S. Matsui, "Multilayer printed circuit board and the manufacturing method," U.S. patent 6,339,197 (15 January 2002).
8. H. Kogelnik, "Coupled wave theory for thick hologram gratings," Bell Syst. Tech. J. **48,** 2909–2947 (1969).
9. M. Z. Zha, P. Amrhein, and P. Gunter, "Measurement of phase-shift of photorefractive gratings by beam-coupling analysis," J. Quantum Electron. **26,** 788–792 (1990).
10. F. Kahmann, "Separate and simultaneous investigation of absorption gratings and refractive-index gratings by beam-coupling analysis," J. Opt. Soc. Am. A **10,** 1562–1569 (1993).